Characterization of Transport through Porous Media with a Crack

E Holzbecher
German University of Technology in Oman (GUtech)

ABSTRACT

Fractured porous media provide an important topic in particular for geologists and for material scientists. Many researchers are concerned with fluid flow. Here we extend the research studies by focussing on transport processes. In order to understand the effect on the micro-scale we examine details of a porous medium with a single fracture, a crack. By numerical experiments using finite element simulations we investigate the effect of crack characteristics on the overall behaviour of the combined flow and transport matrix-crack system that is observed in breakthrough curves. We deal with open cracks and with highly permeable fractures, varying their conductivity in relation to the porous medium conductivity. We also vary the crack orientation relative to the flow direction, and the crack aperture. Aside from the differences between the simulated scenarios, the results show that there is an increased diffusivity with the overall permeability of the system. While the front breakthrough appears earlier for higher permeable cracks, transport in low flow regions is slowed down. As a result, pockets of the replaced fluid remain longer within the system. The latter result can have important implications in application cases.

1. INTRODUCTION

Fractured porous media are of particular interest for geologists, but they are attracting increased attention in the material sciences [1, 2, 3, 4]. They have been studied extensively concerning flow fields and hydraulic properties, experimentally, theoretically and numerically. In geological systems, flow and transport in fractured porous media become more relevant in cases where the deep sub-surface is concerned, where the material is consolidated or has undergone metamorphic processes. In the material sciences fractured porous media are of concern as they are increasingly used as parts of technical devices.

One may distinguish between systems in which only the fractures and their network are relevant, and systems in which both fractures and the matrix with different proportions contribute to overall flow and transport. Here we deal with the latter case. For a basic study of the phenomena, a system with a single fracture is examined. We consider cases in which the fracture is much more permeable than the surrounding and enables preferential flow. For that type of fracture in the sequel we use the term ‘crack’ or ‘fissure’ [5].

While there are many studies on flow in such systems, the effect on transport is much less examined. Here the aim is to highlight some basic features of conservative transport.

*Corresponding Author: ekkehard.holzbecher@gutech.edu.om

Laboratory experiments with such systems are difficult to perform. Numerical experiments have the advantage that basic properties of a crack can be changed easily: the length of the fracture, its orientation, its aperture. The crack itself can be treated as a porous medium, if smaller particles settle within the crack or if chemical precipitation leads to partial clogging. If that is not the case the interior of the crack has to be treated as an open flow region.

Transport in such systems is mainly studied with respect to mass transport, less with respect to heat transport. Berkowitz [6] provided a concise overview on flow and mass transport in geological media. General processes within a system with negligible matrix permeability have been outlined in the reviews of Bodin et al. [7, 8]: advection, hydrodynamic dispersion, matrix diffusion and sorption. The intention here is to cover processes that are relevant for both heat and mass transport. Aside from advection we include only diffusion. The details of dispersion, which is more relevant in solute than in heat transport, are assumed to be of minor relevance, as the system is advection dominated.

The topic has been examined in conjunction with the design of disposal facilities for nuclear waste. The reason for the scrutiny is obvious, if the facility is to be located in fractured rock, as for example in the studies of Mahmoudzadeh et al. [9, 10]. In the same context researchers deal with nuclide migration within cracks in engineered cement barriers [11, 12]. In a verification and validation study Perko et al. [13] compute nuclide breakthrough by numerical modelling. For validation they use an experiment, performed and described by Hull and Clemo [14]. The experiment was performed in a thin (1.25 cm) dual permeability system with several connected fractures sandwiched between two sheets. Using dye, the transport of a tracer plume through fractures and matrix could be visually observed. The figures of the experiment show the fast transport through the fractures, leading to a distortion and elongation of the plume, as well as complex interactions between fractures and matrix. It is the aim of this study to explore the effect of these processes systematically and in detail in a simpler set-up.

Geothermal heat utilization is the motivation for most research on heat transport. Different geometrical constellations have been studied: single fracture in a porous medium [15], simulation of a laboratory study with a simple fracture network in 2D [16], intersecting fractures in 3D [17], geothermal doublets [18], and complex fracture networks [19].

For the modeller there are various options to treat cracks in porous media. Concerning modelling of fluid flow Berre et al. [20] distinguish between discrete fracture matrix networks (DFM) and discrete fracture networks (DFN), aside from single- and multiple continuum approaches. The DFN approach is justified if flow in the matrix can be neglected, while the in DFM one assumes that both matrix and fractures contribute to the entire flux. In respect of transport, a similar distinction can be made. However, the nature of the transport processes makes it less difficult to argue for the neglect of the matrix. Even if only the fractures contribute to fluid flow, matrix diffusion usually plays an important role in mass transport [7, 8]. Also fracture skin might be of importance [21]. Regarding heat transport, this argument against DFN is even more relevant, because thermal diffusion is a process that appears in all media. For these reasons, here the DFM approach is given preference.

By numerical experiments the case of transport in a porous medium with a crack is examined. It shows that global transport through the system differs significantly from the homogeneous case. The problem is investigated by numerical experiments in 2D hypothetical systems with porous and open cracks. We explore the dependency of the breakthrough curves on the crack permeability, thickness, and orientation of the crack.

We examine porous and open cracks. For porous cracks we investigate the role of permeability over several orders of magnitude. We vary the crack aperture, i.e., the ratio between large and small axes, and its angle in relation to the main flow direction. Finally, we extend the 2D study by modelling in 3D.

2. SET-UP AND SCENARIOS

The set-up consists of a single crack within a porous medium (matrix), in 2 and in space dimensions. In 2D the crack is of elliptic shape in a rectangle, in 3D the crack has ellipsoid-shape in a rectangular box. The boundary conditions are chosen in a way that in the constellation without the crack would induce a 1D constant flow field. A difference of hydraulic head ΔH is fixed on opposite sides, while there are no-flow conditions on the other sides. The main axis of the crack is much longer than the smallest axis. In 3D the intermediate axis is slightly smaller than the main axis. The largest axis of the ellipse forms an angle α with the flow. Figure 1 depicts the geometry of the 2D model region for an angle of 45° and an axes-ratio of $d = 10$.

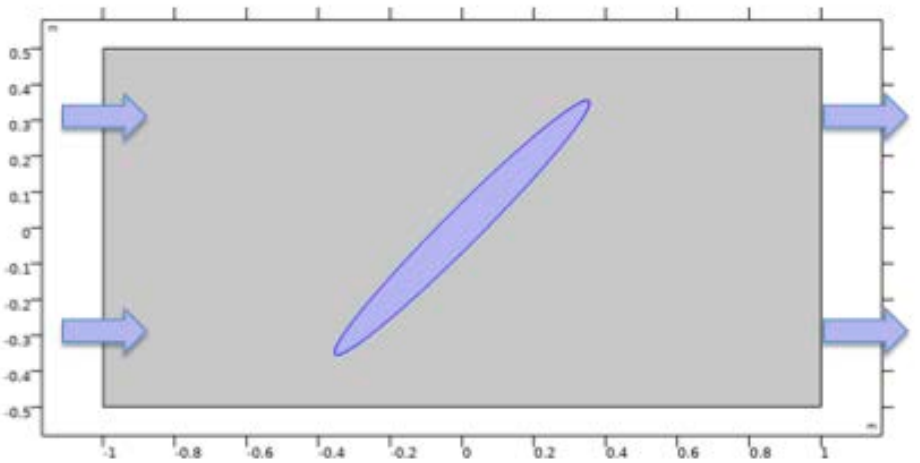

Figure 1: Sketch of a crack in a porous medium, as treated here; flow is from left to right

For the matrix we assume Darcy's Law with a low permeability. Concerning the flow in the crack we consider various constellations. If there are no obstacles within the crack, if there is free flow, the Navier-Stokes's equations are assumed to be valid to describe laminar flow within the free space. If the crack itself is filled, or partially filled, with porous material of smaller size, one can assume Darcy's Law within the crack, with a permeability that is much higher than that of the matrix. An intermediate way of mathematical formulation between the two mentioned descriptions is given by the Brinkman equations, in which free fluid flow and porous media flow are combined. It is the advantage of the Brinkman equations that depending on the local variable size, the dominance of either one or the other regime is automatically taken into account. In the following the details of these alternatives are briefly presented, introducing the relevant parameters.

For the porous matrix the validity of Darcy's Law is assumed, which states that the velocity is proportional to the gradient of the hydraulic head. Corresponding to the hydraulic head one may use the pressure p, which is derived from the total pressure by eliminating the hydrostatic part at depth z: $p = p_{total} - \rho g z$. Darcy's Law and the continuity equation as the expression of mass conservation led to a differential equation for p:

$$\nabla \frac{k}{\mu} \nabla p = 0 \tag{1}$$

with permeability k and dynamic viscosity μ. For the matrix-crack system we use a spatial dependence of k, k_{low} in the matrix and k_{high} in the crack:

$$k(x,y) = \begin{cases} k_{low} & in\ the\ matrix \\ k_{high} & in\ the\ porous\ fracture \end{cases} \tag{2}$$

For the parameter variations we define the ratio between the conductivities:

$$k_{ratio} = \frac{k_{high}}{k_{low}} \tag{3}$$

At high velocities Darcy's Law may not be valid anymore and a nonlinear relation between velocity and hydraulic head becomes valid. This is considered in the Brinkman equations [22]:

$$\begin{gathered} \frac{\mu}{k}\boldsymbol{v} + \nabla p - \nabla \frac{\mu}{n}(\nabla \boldsymbol{v} + (\nabla \boldsymbol{v})^T)) = 0 \\ \nabla \cdot \boldsymbol{v} = 0 \end{gathered} \tag{4}$$

where n denotes porosity. Dependent variables in the Brinkman formulation are the pressure p and the components of the velocity vector $\boldsymbol{v}$. For low velocities the formulation (4) yields Darcy's Law, while for high velocities it approximates the Navier-Stokes's equations for fluid flow (see below).

As a limit situation we consider also the case of open cracks, where Darcy's law or the Brinkman extension are not valid anymore. As flow in the considered systems is usually low, we assume that the flow in the cracks is laminar. Steady laminar flow can be described by the Navier-Stokes's equations

$$\begin{gathered} \rho(\boldsymbol{v}.\nabla)\boldsymbol{v} + \nabla p - \nabla \mu(\nabla \boldsymbol{v} + (\nabla \boldsymbol{v})^T) = 0 \\ \nabla \cdot \boldsymbol{v} = 0 \end{gathered} \tag{5}$$

where ρ denotes density. Usually, the first term that accounts for inertia effects is neglected and the equation reduces to Stokes's flow [23]. If the corresponding term in the Brinkman equation (4) is neglected and the crack is open (n = 1), one also obtains Stokes's flow.

Mass and heat transport can be described by the same advection-diffusion equation that can be written as:

$$\frac{\partial \theta}{\partial t} = \nabla \boldsymbol{D} \nabla \theta - \kappa \boldsymbol{v} \nabla \theta \tag{6}$$

The variable θ represents concentration in the case of solute transport and temperature in the case of heat transport. The factor κ in the advection term is relevant only for heat transport, where it denotes the ratio of specific heat capacities $\kappa = (\rho C)_f / (\rho C)_{fs}$. The (ρC) terms denote the heat capacities where the subscripts refer to the fluid (f) and the fluid-solid (fs) phases. For solute mass transport, the equation (6) holds with $\kappa = 1$. $\boldsymbol{D}$ generally, denotes the dispersion tensor, in 2D given by

$$\boldsymbol{D} = (D + \alpha_T v)\boldsymbol{I} + \frac{\alpha_L - \alpha_T}{v} \boldsymbol{v}\boldsymbol{v}^T \tag{7}$$

The values for the diffusivity D are quite different for solute and thermal transport. For thermal transport the values are in the order of $10^{-6}\ m^2/s$, whereas in mass transport they are in the order of $10^{-9}\ m^2/s$. Thus, the dispersive velocity dependent term is much more important in solute transport than in heat transport. In this paper, we focus on advection dominated transport. For that reason, we neglect the details expressed in equation (7) and consider a scalar diffusivity value D instead of the complete tensor.

In this paper, we assume that effects of variable density are not relevant. For an examination the models would have to be extended by a back-coupling, as flow can be affected by the distribution of the transport variable [24].

Table 1: Parameters for the reference case and variations in parametric sweeps

Parameter	**Unit**	**Symbol**	**Reference Value**	**Variation**
Crack length	-	L	1	-
Crack aperture	-	d	0.02	$\frac{1}{160}, \frac{1}{80}, \frac{1}{40}, \frac{1}{20}, \frac{1}{10}$
Angle between crack axis and flow direction	-	α	$\frac{\pi}{4}$	$0, \frac{\pi}{8}, \frac{\pi}{4}, \frac{3\pi}{8}, \frac{\pi}{2}$
Matrix permeability		k_{low}	10^{-4}	-
Crack permeability (for porous cracks)		k_{high}	10^{-2}	10^{-4}, 10^{-3}, 10^{-2}, 10^{-1}, 1
Fluid viscosity	$Pa\ s$	μ	0.001	-
Fluid density	kg/m^3	ρ	1000	-
Matrix porosity	-	n	0.25	-
Crack porosity	-	n	0.25	-
Matrix diffusivity	-	D	10^{-4}	-
Head difference	-	ΔH	1	-
Heat capacity ratio	-	κ	3	-

For a general treatment of the problem, the system is normalized. For the space variables we use the reference length L. Here we choose the long axis of the crack as length unit L. With the time transformation $t \rightarrow t \cdot D/L^2$ the transport equation with the scalar coefficient D can be written in dimensionless form, as:

$$\frac{\partial \theta}{\partial t} = \nabla^2 \theta - Pe \cdot \boldsymbol{v} \cdot \nabla \theta \tag{8}$$

with Peclet number Pe defined by:

$$Pe = \begin{cases} \frac{v_0 L}{D_{sol}} & for\ solute\ transport \\ \frac{\kappa v_0 L}{D_{therm}} & for\ heat\ transport \end{cases} \tag{9}$$

With Pe = 150 in the reference scenario in our simulations, diffusive processes are negligible in comparison to advection, in the crack as well as in the matrix. For the system there remain three dimensionless ratios of relevance: d/L, k_{ratio} and α. These are the parameters that are varied systematically in order to obtain a general impression of the system's behaviour.

3. NUMERICAL MODEL

The model set-up represents a situation in which a fluid with a certain transport property displaces a fluid with a different value for that property. Thus, cases of thermal transport are covered in which a cold fluid penetrates into a warmer fluid, in which a hot fluid replaces a colder one, but also cases of solute transport in which a fluid with a certain concentration of a biogeochemical species moves into a system with a different initial concentration. The modelling reveals how the pattern of a front with an initially equal penetration breaks down when the crack is approached.

The models were set up using the commercial software COMSOL Multiphysics (version 5.6), an implementation based on the Finite Element method. Because of its versatility the software is applied in many technical and scientific fields. Several publications demonstrate the feasibility of the program to simulate multi-physics processes in fractured media [11, 12, 13, 18, 25, 26, 27]. Here we utilize various modes for fluid flow and transport.

For the computation of the steady flow field several options of the software were used. The Darcy mode (esdl) was applied for simulations with porous cracks, solving eq. (1) with permeabilities k_{low} and k_{high} respectively. We also applied the Brinkman mode (chns) for highly permeable cracks, described by eq. (4). For open cracks the free and porous media (fp) was implemented, which uses the Navier-Stokes's equations (5) in the crack. We examined the option to neglect the inertial term, which describes Stokes's flow.

For transport the advection-diffusion equation (6) is solved. In the simulations we use a dimensionless variable θ. The simulations thus cover the cases of solute and thermal transport. The initial condition prescribes a value of in the entire model.

The inflow is described by the boundary condition $\theta = 0$ (in the figures at the left boundary). For the thermal case with cold fluid replacing hot fluid θ is defined by:

$$\theta = \frac{T - T_{low}}{T_{high} - T_{low}} \tag{10}$$

For the solute case with a high concentration entering a low concentration region it is given by:

$$\theta = \frac{c_{high} - c}{c_{high} - c_{low}} \tag{11}$$

There is a one-way coupling between the transport equation and the flow equations. The solutions of the steady-state flow fields are stored and used in the simulation of transient transport.

In all simulations irregular triangular meshes with quadratic elements were generated. The meshes were drastically refined near and inside the crack. Figure 2 depicts details of an example mesh. As an example, the mesh for the reference model consists of 6046 elements and 3072 nodes. The number of degrees of freedom (DOF) in the model for flow and transport is 12189. The mesh of the 3D model consists of 1456911 tetrahedra and 244920 nodes.

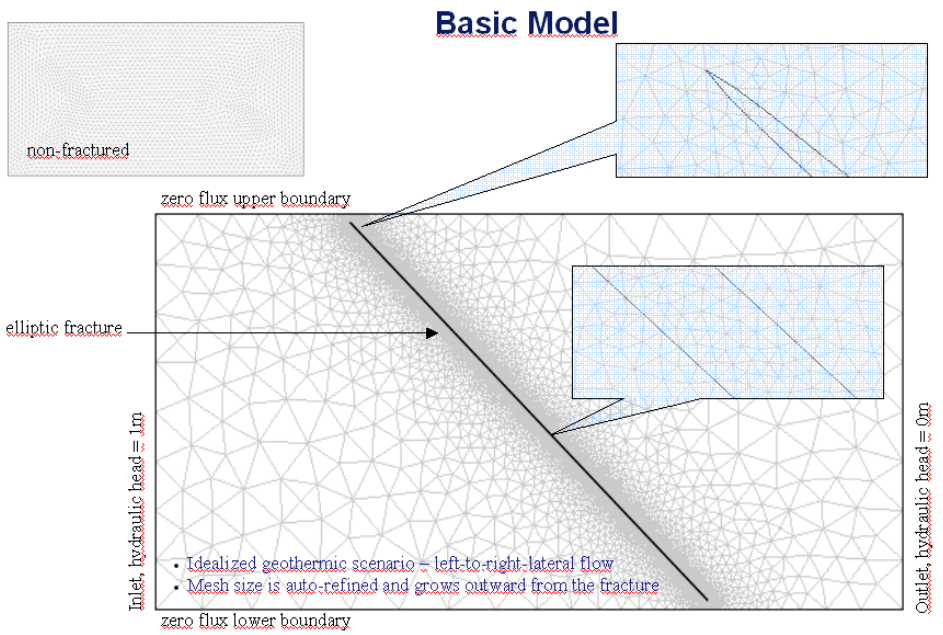

Figure 2: Reference 2D model with an elliptic crack, set-up and Finite Element mesh

4. RESULTS

4.1. 2D Transport Pattern

In absence of the crack, in a 1D flow, the inflowing fluid would move through the system in a front with no deviations in the transverse direction. This simple pattern disappears if there is a highly permeable crack. The influence of the crack is visualized in the following.

Figure 3 with its sub-plot demonstrates the details of transport in the vicinity of the crack. The flow field is represented by a flow net of streamlines and pressure contour lines. As the size of a quadrilateral is an indicator of velocity size, zones of fast and slow flow can be identified visually. At the tips of the cracks the velocities are highest. There is slow flow backstream of the crack front end, and upstream of the crack back end. This characteristic flow field has implications on the transport.

In the plots the fluid that is entering from the left is depicted in blue, while the replaced fluid is visualized in red (imagine a cold fluid replacing a hot one!). Other colours visualize mixed fluid. The figure shows the distribution of the transport variable at four-time instances. In the first the moment is captured, when the intruding front has just reached the crack front tip. The enhanced transport inside the crack due to fast flow is clearly visible. The following plots show the development of a blue area downstream from the crack indicating the dominance of the intruding fluid. This area is constantly widening and finally covers a wide part in the centre of the outlet on the right, as depicted in the last subplot. However, at the upper and lower margins, pockets of the initial fluid remain for a long time. The appearance of these pockets is clearly related to the slow flow zones that were indicated earlier.

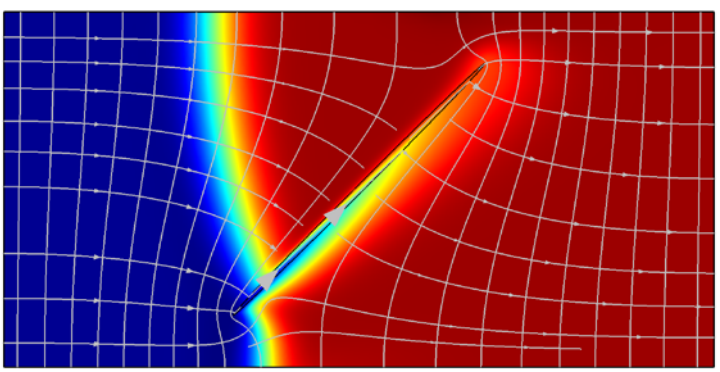

(a)

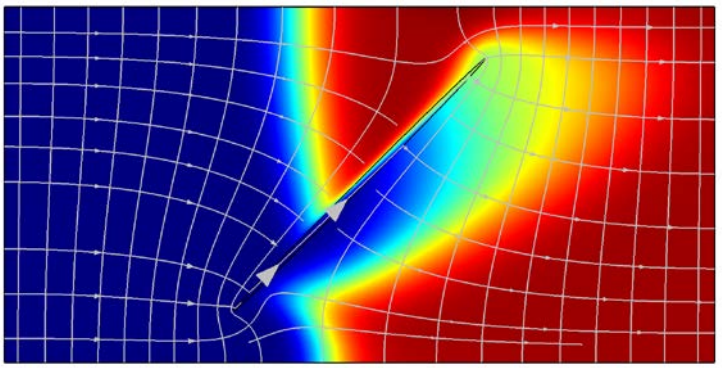

(b)

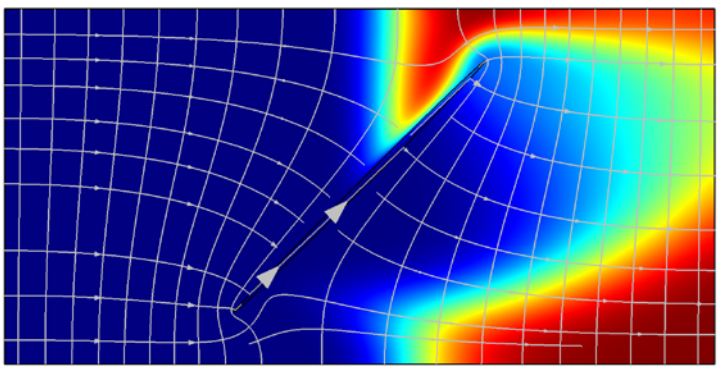

(c)

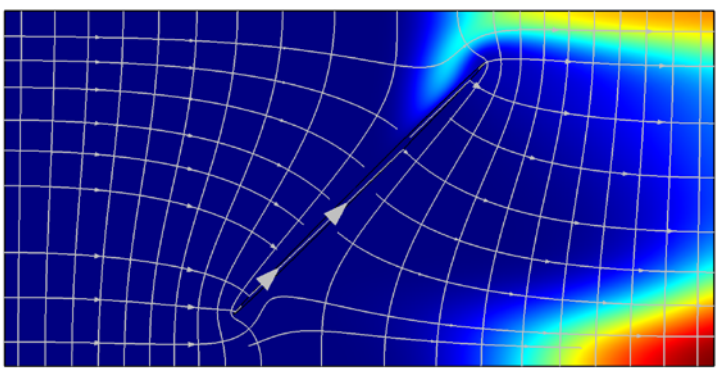

(d)

Figure 3: Transport sequence for reference set-up (at dimensionless times t = 40, 60, 90, 120), k_{ratio} = 1000, d = 1/50

4.2. Breakthrough Curves

The effect of the observed phenomena of the transport process can be examined on the breakthrough curves. The advective outflow $j(t)$ is computed by integration along the outflow edge:

$$j(t) = \int v_n \cdot \theta(t) dn \tag{12}$$

The evaluation of equation (12) is not related to a single location but yields a breakthrough for the entire outflow. It could be termed as an 'effective breakthrough', similar to an effective property, for example an effective conductivity, as computed in studies on flow in fractured media [28, 29]. While in steady state the effective permeability or conductivity is represented by a single value, one obtains a time-dependent curve in the unsteady situation of a passing front.

In the simulations the initial fluid is characterized by $\theta = 1$, while there is an inflow (Dirichlet) boundary condition $\theta = 0$.Thus the breakthrough curves at the outflow show a high value initially (that represents fluid flow, as the θ in eq. (12) equals 1) and decreases to zero while the front penetrates into the system.

Figure 4 depicts resulting breakthrough curves for different values of the permeability ratio k_{ratio}. k_{ratio} was increased by factors of 10 between 1 (homogeneous case) and 104. In the latter case the crack is 10000 times more permeable than the surrounding. The curve for $k_{ratio} = 1$ represents the reference breakthrough in a homogeneous medium. The graph clearly shows the effect of the crack on the transport process.

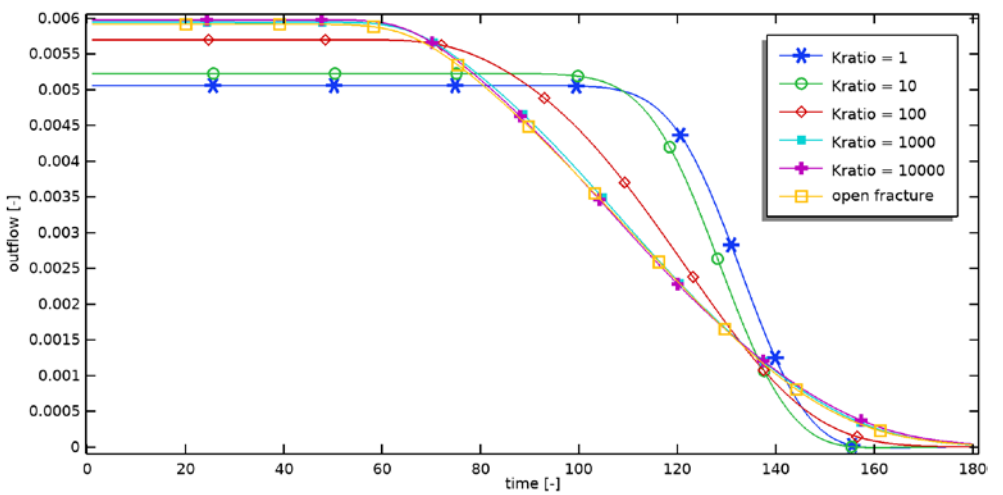

Figure 4: Breakthrough curves for reference set-up; dependence on permeability ratio

Firstly, one can observe an increasing outflow of the initial fluid. This is due to the higher fluid velocities when the crack is more permeable. For higher k_f and thus k_{ratio} there will be higher velocities, which lead to a higher advective flux also at the outlet. Secondly one observes a higher diffusivity: the steep slope of the breakthrough curve for the homogeneous case is replaced by smaller gradients. The gradients clearly decrease with increasing crack permeability. As one consequence the replaced fluid remains longer in the system, if k_{ratio} is higher. The higher diffusion is an effect of the pockets of increased concentration that remain longer in the low velocity regions. The third effect is acceleration. Obviously, the mass midpoints arrive earlier at the outlet if the permeability is higher. The strongest contrast can be observed between breakthrough curves for k_{ratio} = 10 and 100. This is also an effect of the increased mean velocity.

Finally, it is to see that there is no effect of crack ratio above the value of 1000. Breakthrough for k_{ratio} =1000 and = 10000 are identical. The constraints within the thin structure of the high permeable crack do not lead to a recognizable change in the transport processes.

For comparison we performed runs with an open crack, in which the flow can be described by the Navier-Stokes's equations (5). Here we used the options to consider or neglect the inertial terms. In addition, the Brinkman formulation was tested, also with the same options. The corresponding flow patterns and breakthrough curves for all of these alternatives fit almost completely with the ones for the high permeable porous cracks.

One can expect that flow and transport strongly depend on the angle that the crack forms with the flow direction. In order to investigate this the model was run with crack angles of 0°, 22.5°, 45°, 67.5° and 90°. A zero-degree angle represents the case, in which the crack is aligned with the flow. For a 90° angle the crack is perpendicular to the flow. Figure 5 depicts the breakthrough curves. As expected, the flow is the highest for the 0° case and decreases with an increasing angle. This is clearly reflected in the initial advective outflux, and also in the breakthrough of the mass centre. Remarkably, the shape of the breakthrough curves changes considerably. While they have the common outlook for angles of 45° and larger, they change to a convex-concave shape for low angles. This behaviour can be explained easily: when the front reaches the front tip of the crack the increased advective flux leads to a more rapid change (here: drop) of the transport variable. There is the opposite effect at the back tip of the crack, where reduced gradients can be observed. Near the end of the simulated time period the scenario with the aligned crack even shows the highest concentrations. This makes sense, if one recognizes that the flow in the porous part of the system is lowest in this situation.

In another parametric sweep the effect of the crack thickness d has been examined. The results for k_{ratio} =100 and an angle of 45° are shown in Figure 6. As expected, the total flow through the matrix-crack system increases with the crack width d. When the front passes the crack, after half of the shown time period, the effect on the breakthrough is higher if the crack is wider. A finding that is less expected is that in the long run the remnants of the initial fluid remain longer in the system, if d is larger. Similarly, to the previously discussed cases this can be attributed to the fact the velocities in the low permeable matrix are smaller for the wide crack, causing a slower advection in those parts.

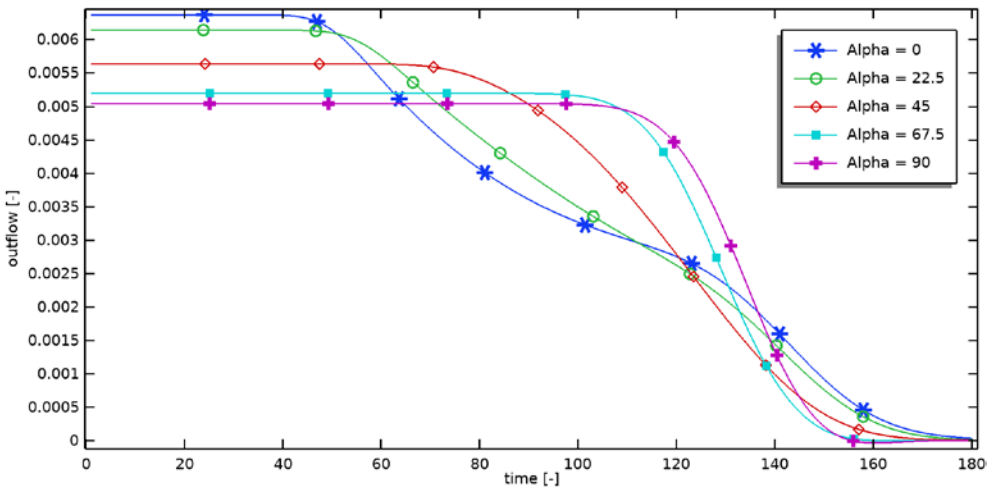

Figure 5: Breakthrough curves for reference set-up; dependence on crack angle; k_{ratio} = 100.

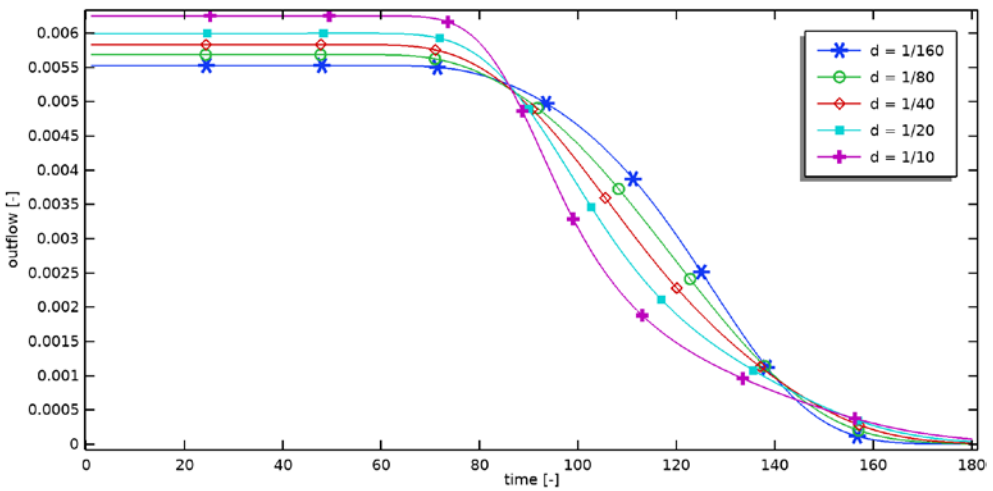

Figure 6: Breakthrough curves for reference set-up; dependence on crack thickness

4.3. 3D Simulation

For an examination of the 3D case a model with a single ellipsoid fracture was set up. The boundary conditions are prescribed in a way that in the absence of the crack they would induce a 1D flow (in x-direction) Then the inflowing fluid would penetrate into the system in a front with no deviations in transversal directions. We show results for a constellation with a crack that lies with its main axis at a 45° angle with the main flow direction. A selected output of the coupled flow and transport model, using COMSOL Multiphysics, is shown in Figure 7. The ellipsoidal crack can be recognised in the middle of the system.

The plot depicts the distribution of the transport variable at a time instance when the front passes the fracture. Grey lines show streamlines. The initially present fluid is indicated by red colour. The incoming fluid is plotted in blue. Intermediate colours show the mixing, i.e., the distorted position of the front. Three cross-sections in flow direction are selected to visualise the complex distribution of the transport variable.

At the chosen time instant the front has already passed the upstream tip of the crack. In the middle of the front cross-section the movement is obviously retarded, leading to a deviation heading upstream. The middle cross-section shows a completely different behaviour. The front has advanced further, except at the upper and lower boundaries. The cross-section near the downstream tip of the crack shows the fastest movement of the fluid, as some inflowing fluid almost reaches the outflow boundary. But that holds only in the middle of the cross-section. There are pockets of the initial fluid left behind, at the upper and lower boundaries, and most importantly, upstream of the crack.

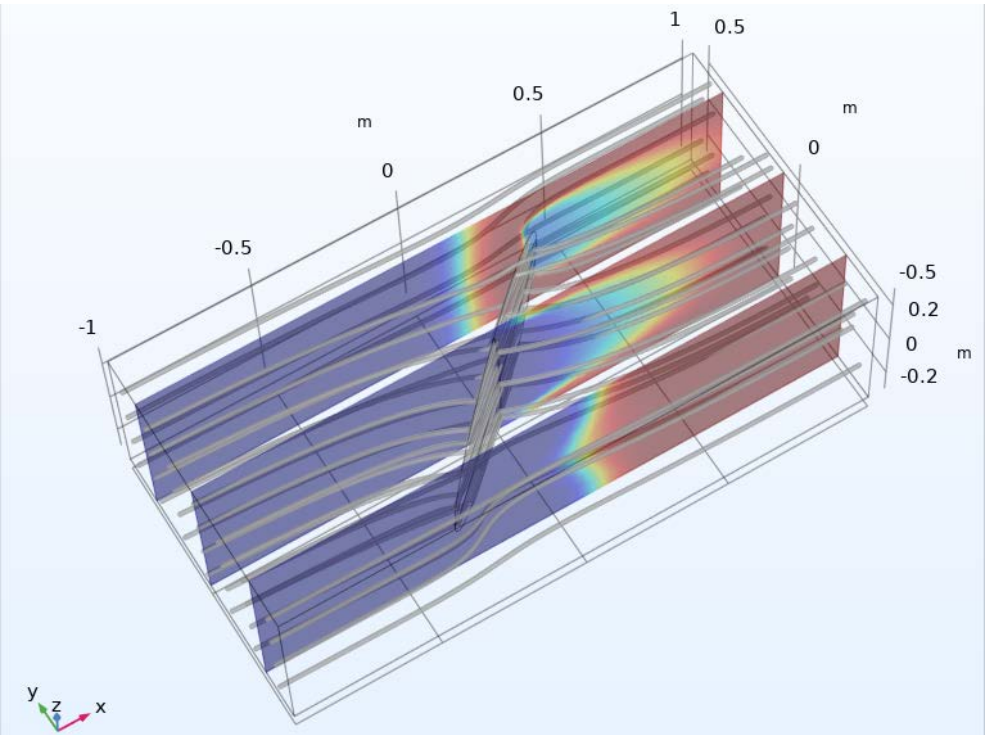

Figure 7: Distribution of transport variable while passing a crack in 3D

The observations can be understood easily. In general, the incoming fluid moves fastest at middle depth, where the crack has its largest extension. Following the fastest pathway fluid particles leave the crack near the back-stream end of the crack and approach the outlet boundary in the shortest time. Near the upper and lower boundary, the fluid has no partial passage through the crack and thus it is slowest. There are pockets of initial fluid that remain in the system for a longer time. These are connected with low velocity parts of the system and lead to the different type of front in the front cross-section (where there is a slow region behind the crack), and to left behind fluids in the back cross-section (where the slow region appears upstream of the crack).

Altogether the behaviour of the transport variable while passing the crack reproduces several features that were already observed in the 2D case.

5. SUMMARY AND OUTLOOK

A fluid system with a low permeable matrix including a highly permeable crack was investigated using numerical experiments, with focus on the effects on conservative transport. Breakthrough curves have been examined systematically using parametric sweeps on the crack permeability, the angle between crack axis and flow direction as well as the crack thickness. We compared constellations with a porous crack as well as an open crack.

The simulated scenarios showed various effects on the breakthrough: an increase of advective transport, of acceleration in comparison to the homogeneous case and an increase of effective diffusion. Generally, it was observed that parameters that increase the flow in the crack have three major effects. In comparison to the homogeneous system: (1) they increase the overall fluid flux, (2) they lead to an earlier breakthrough, (3) remnants of the initial fluid remain longer in the system. For solute transport the dispersion at the local scale, represented in the dispersion tensor, may aggravate the here observed effects.

The effects observed here are most pronounced in variation of crack permeability. A distortion of the usual breakthrough type curve is mainly observed in variations of the crack orientation, and most pronounced in constellations in which the long crack axis is aligned with the direction of fluid flow.

Using various free flow approaches for the crack in the simulations we conclude: (1) an open crack can be seen as the limit case of a highly permeable crack. Flow and transport in a system with a highly permeable crack (k_{ratio} > 1000) and in a system with an open crack show only marginal difference. (2) Inertial effects are not relevant for a crack.

Here focus lay on basic conservative transport processes, advection and diffusion. Further parameters come into play if dispersion, degradation and/or chemical reactions are considered. Using the proposed methods, the study can be extended for the examination of these processes in more complex constellations, as for example of crack networks in 2D and 3D. However, detailed studies on networks are restricted by requirements on mesh size limits. In 2D large fracture networks may require meshes with too many nodes. In 3D even models with a few cracks require extremely refined meshes to capture details at intersections.

REFERENCES

[1] Sahimi, M., Flow and Transport in Porous Media and Fractured Rock: From Classical Methods to Modern Approaches 2011. Wiley & Sons, Hoboken.

[2] Adler, P.M., Thovert, J.-F., Mourzenko, V.V., Fractured Porous Media 2013. Oxford Univ. Press, Oxford.

[3] National Academies of Sciences, Engineering, and Medicine, Characterization, Modeling, Monitoring, and Remediation of Fractured Rock 2015. The National Academies Press, Washington, DC.

[4] Lui, R., Jiang, Y., Special issue: fluid flow in fractured porous media, Processes 2018. 6, 178,

[5] Peacock, D.C.P., Nixon, C.W., Rotevatn, A., Sanderson, D.J., Zulaga, L.F., Glossary of fault and other crack network, Journal of Structural Geology 2016. 92, 12-29.

[6] Berkowitz, B., Characterizing flow and transport in fractured geological media: a review, Advances in Water Resources 2002. 25, 861–884,

[7] Bodin, J., Delay, F., de Marsily, G., Solute transport in a single fracture with negligible matrix permeability: 1. fundamental mechanisms, Hydrogeology Journal 2003. 11, 418–433,

[8] Bodin, J., Delay, F., de Marsily, G., Solute transport in a single fracture with negligible matrix permeability: 2. Mathematical formalism, Hydrogeology Journal 2003. 11, 434–454,

[9] Mahmoudzadeh, B., Liu, L., Moreno, L., Neretnieks, I., Solute transport in fractured rocks with stagnant water zone and rock matrix composed of different geological layers – model development and simulations, Water Resources Research 2013. 49, 1709–1727,

[10] Mahmoudzadeh, R., Solute Transport through Fractured Rocks: the Influence of Geological Heterogeneities and stagnant Water Zones, Doctorate Thesis 2016. Royal Inst. of Tcchnology, Stockholm, ISBN 978-91-7595-906-1

[11] Perko, J., Seetharam, S.C., Jacques, D., Mallants, D., Cool, W., Vermarien, E., Influence of cracks in cementitious engineered barriers in a near-surface disposal system: assessment analysis of the Belgian case, 15th Int. Conf. on Env. Remediation and Radioactive Waste Management (ICEM2013) 2013. Paper ICEM2013-96226.

[12] Seetharam, S.C., Perko, J., Jacques, D., Mallants, D., Influence of fracture networks on radionuclide transport from solidified waste forms, Nuclear Engineering and Design 2014. 270, 162–175,

[13] Perko, J., Seetharam, S., Mallants, D., Verification and validation of flow and transport in cracked saturated porous media, COMSOL Conf. 2011, Stuttgart.

[14] Hull, L.C., Clemo, T.M., Dual-permeability model: laboratory and FRACSL validation studies, in: Geothermal Injection Technology Program Annual Progress Report FY-86, EGG-2511, 1987. Idaho National Engineering, Laboratory, Idaho Falls.

[15] Bagalkot, N., Kumar, G.S., Thermal front propagation in variable aperturefracture–matrix system: A numerical study, Sādhanā 2015. 40(2), 605-622.

[16] Pastore, N., Cherubini, C., Giasi, C.I., Allegretti, N.M., Redondo, J.M., Tarquis, A.M., Experimental study of heat transport in fractured network, Energy Procedia 2015. 76, 273-281,

[17] Jacquey, A.B., Cacace, M., Blöcher, G., Modelling coupled fluid flow and heat transfer in fractured reservoirs: description of a 3D benchmark numerical case, Energy Procedia 2017. 125, 612-621,

[18] Jarrahi, M., Moore, K.R., Holländer, H.M., Comparison of solute/heat transport in fractured formations using discrete fracture and equivalent porous media modeling at the reservoir scale, Physics and Chemistry of the Earth 2019. 113, 19-21,

[19] Gisladottir, V. R., Roubinet, D., Tartakovsky, D.M., Particle methods for heat transfer in fractured media, Transport in Porous Media 2016. 115(2), 31-16,

[20] Berre, I., Doster, F. Keilegavlen, E., Flow in fractured porous media: a review of conceptual models and discretization approaches, Transport in Porous Media 2019, 130, 215-236,

[21] Natarajan, N., Kumar, S., Numerical modeling of solute transport in a coupled sinusoidal fracture matrix system in the presence of fracture skin, Int. Journal of Energy and Environment 2010. 4(4).

[22] Brinkman, H.C., A calculation of the viscous force exerted by a flowing fluid on a dense swarm of particles, Appl. Sci. Res. A1 1947, 27-34.

[23] Guyon, E., Hulin, J-P., Petit, L., Hydrodynamik 1997. vieweg, Braunschweig, ISBN 978-3-322-89831-9

[24] Holzbecher, E., Convective Transport through Porous Layers, Int. Journal of Multiphysics 2020. 14(1), 53-67.
[25] Holzbecher, E., Wong, L., Litz, M.-S., Modelling flow through cracks in porous media, COMSOL Conf. 2010, Paris.
[26] Romano-Perez, C.A., Diaz-Viera, M.A., A comparison of discrete crack models for single phase flow in porous media by COMSOL Multiphysics® software, COMSOL Conf. 2015, Boston.
[27] Lugo-Mendez, H.D., Valdes-Parada, F.J., Porter, M.L., Wood, B.D., Ochoa-Tapia, J.A., Upscaling diffusion and nonlinear reactive mass transport in homogeneous porous media, Transport in Porous Media 2015. 107, 683–716,
[28] Rivard, C., Delay, F., Simulations of solute transport in fractured porous media using 2D percolation networks with uncorrelated hydraulic conductivity fields, Hydrogeology Journal 2004. 12, 613-627,
[29] Holzbecher, E., Statistics of numerical experiments with multi-crack systems, COMSOL Conf. 2020, Boston.